Dyes and Pigments 92 (2011) 749–757

Contents lists available at ScienceDirect

Dyes and Pigments

journal homepage: www.elsevier.com/locate/dyepig

New 2,2-difluoro-1,3,2(2*H*)oxazaborines and merocyanines derived from them

Konstantin Zyabrev*, Marina Dekhtyar, Yurii Vlasenko, Alexander Chernega, Yurii Slominskii, Aleksei Tolmachev

Institute of Organic Chemistry, National Academy of Sciences of Ukraine, 5 Murmanska Str., 02660 Kyiv, Ukraine

ARTICLE INFO

Article history:
Received 7 April 2011
Received in revised form
24 May 2011
Accepted 28 May 2011
Available online 13 June 2011

Keywords:
Absorption
Dioxaborine
Fluorescence
Merocyanine
Oxazaborine
X-ray diffraction

ABSTRACT

Synthetic methods have been developed to prepare oxazaborines, the azaanalogues of 2,2-difluoro-1,3,2(2*H*)dioxaborines, which can form merocyanine dyes. The first oxazaborine merocyanines with the isomeric position of the coordinating nitrogen atom have also been obtained. Comparing the spectral properties of donor-acceptor dioxa- and oxazaborine dyes, it is seen that substitution of the 3-O atom by the NH group in the chelate ring has a slight effect on absorption and fluorescence band positions but causes the intensity redistribution between the 0–0 and 0–1 vibronic absorption peaks and thus induces a change in the absorption band shape due to the enhanced solvation of oxazaborines. Substitution of the 1-O ring atom by the NPh group leads to a bathochromic shift and a manifold increase in the fluorescence quantum yield for the corresponding boron chelate dyes.

1. Introduction

2,2-Difluoro-1,3,2dioxaborine polymethine dyes are of considerable current interest due to their applications in NLO [1] and OLED materials [2] as well as in two-photon absorption processes [3]. π-Conjugated systems incorporating boron chelates are remarkable for their flexible molecular design and feasible synthesis which afford a great diversity of dye types. As an example, 2,2-difluoro-1,3,2(2*H*)dioxaborines give rise to anionic and zwitterionic polymethines [1a,4,5] as well as to typical merocyanines [1b,6,7], linear [2a], and star-shaped uncharged π-compounds [2d,e,3a].

The spectral properties of quasi-linear dyes including those containing BF_2 complexes are dictated by the constitution of heterocyclic end groups and the π-linker between them. Previously we investigated the relationship between the structure of the polymethine chain and the spectral behavior of dioxaborine dyes [4]. Ligand variations in π-conjugated compounds of O,O-chelated boron and their effects on the corresponding dye spectra have also been thoroughly studied (see Refs. 1–7 and the works cited therein). Further, the colour theory states that heteroatom substitutions in dye auxochromes can cause significant spectral effects [8]. At the same time, there has been no reported evidence of the relationship between the nature of the coordinating atom and the spectral properties of boron chelate polymethine compounds. Aiming at spectral controllability of π-conjugated chelate systems, here we address the optical effects caused by the O-to-N substitution in the ligands of boron chelate dyes. It should be noted that a number of visible-absorbing and intensely fluorescing π-conjugated oxazaborine systems have recently been described [9]. They were synthesized by suitable tailoring of the ligand with a highly developed π-conjugated system followed by the chelation of the BF_2 group to give the target coloured compounds. In the present work, we have developed a more general and convenient synthetic approach to oxazaborine dyes which involves first the synthesis of the N,O-chelate and then the extension of the polymethine chromophore like in conventional cyanine chemistry.

2. Results and discussion

As model and reference compounds, we have used the boron complex of 2-acetyldimedone **1** and related unsymmetrical dyes **2** and **3** synthesized by us previously [10] (Fig. 1)

A rationale for this choice is that the exocyclic carbonyl group conjugated with the chelate ring, activates the coordinating carbonyl groups towards amines, just as α-trihaloalkyl substituents do [11]. In addition, 2-acetyldimedone is a convenient starting reagent to prepare isomeric N,O-coordinating ligands which, as

* Corresponding author. Tel.: +380 44 5510682; fax: +380 44 5732643.
E-mail address: zyabrev@ukr.net (K. Zyabrev).

0143-7208/$ – see front matter © 2011 Elsevier Ltd. All rights reserved.
doi:10.1016/j.dyepig.2011.05.025

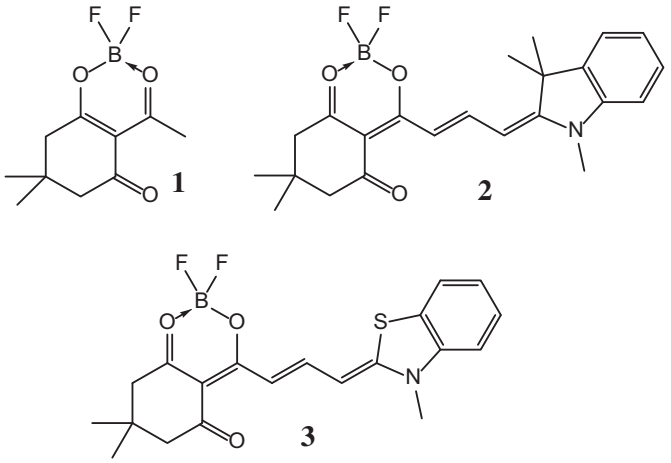

Fig. 1. Boron chelate **1** and related unsymmetrical dyes **2** and **3**.

shown later, are further involved in the synthesis of key oxazaborines.

To obtain oxazaborine polymethine dyes, we attempted the classical method based on the recyclization of 4-pyrylo- to 4-pyridocyanines [12]. The corresponding reaction with amines is quite typical for 2,2-difluoro-1,3,2(2*H*)dioxaborines [13]. However, as found, merocyanines **2** and **3** are unreactive to both weakly basic (aniline, *p*-anisidine) and highly basic amines (benzylamine, methylamine) whereas chelate **1** recyclizes under the same conditions to oxazaborine **4** in high yield (Scheme 1).

The attempted reaction of boron complex **4** with various electrophiles did not proceed, in accordance with the literature data [13]; an electrophilic attack on the methyl group is likely to be hindered by the spatially close carbonyl and phenyl groups. The steric hindrances in the oxazaborine nucleus are avoided in complex **6** containing no phenyl substituent. As a result, it has been successfully reacted with the benzothiazole-derived conjugated ω-aldehyde to provide unsymmetrical dye **7** (Scheme 2).

To obtain the isomeric oxazaborine, 2-acetyl-3-amino-5,5-dimethylcyclohex-2-enone **8** was treated with boron trifluoroetherate; disappointingly, the expected chelation failed to occur, as it stopped at the stage of complex **9**. Even the use of sterically hindered strong bases (such as DBU and *N*,*N*-diisopropylethylamine) as HF-abstracting agents was unsuccessful (Scheme 3).

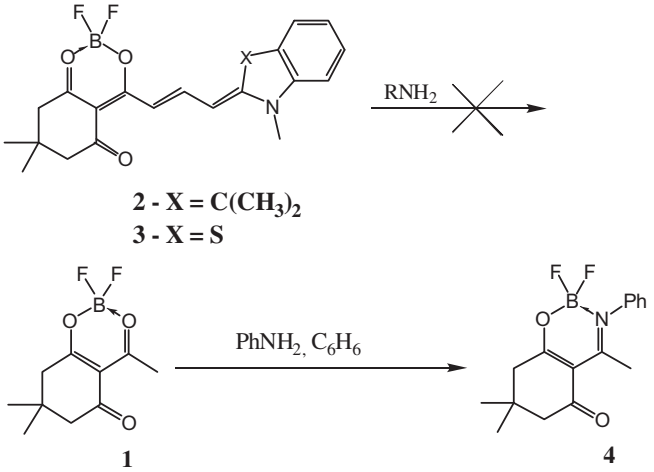

Scheme 1. Reactions of **1**–**3** with amines.

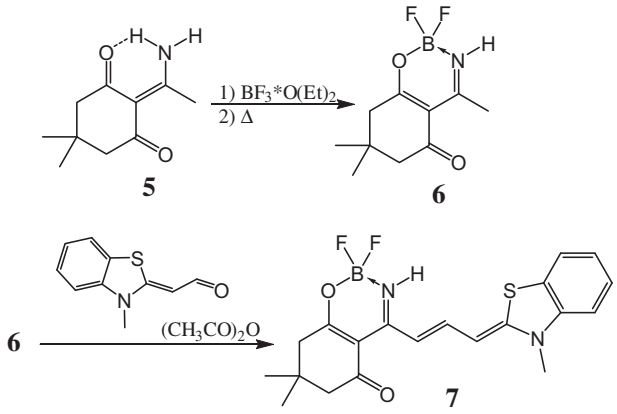

Scheme 2. Synthetic route to oxazaborine dye **7**.

Compound **9** cannot form a chelate presumably due to the decreased electrophilicity of the boron atom which, in turn, may result from the relatively high nucleophilicity of the amino group in ligand **8** (as compared to its isomer **5**). The amino group nucleophilicity was sufficiently lowered on passing from compound **8** to its phenyl-substituted derivative **10**, so that the latter afforded chelate **11**. The α-methyl group in its oxazaborine ring proved active enough to yield merocyanines **12** and **13** by condensations with appropriate heterocyclic ω-aldehydes (Scheme 4).

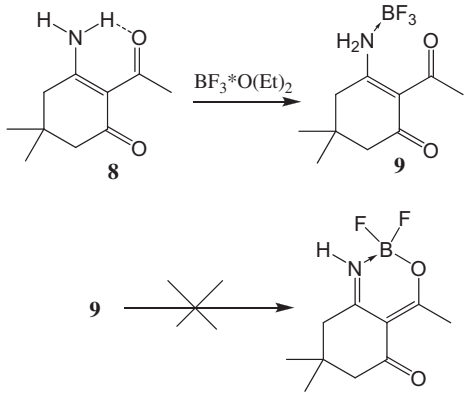

Scheme 3. Reaction of enamine **8**.

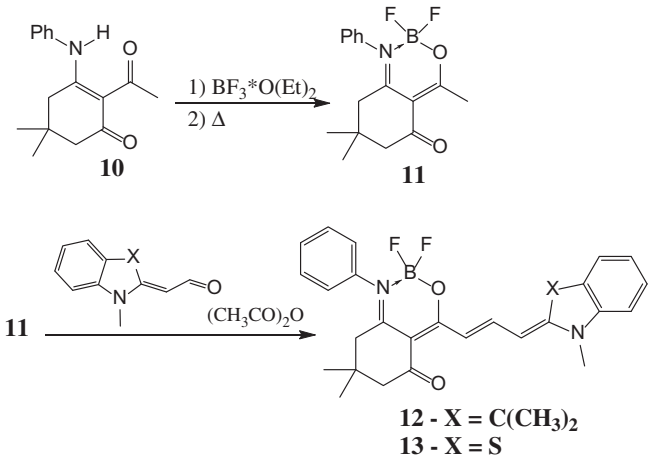

Scheme 4. Synthesis of oxazaborine **11** and related unsymmetrical dyes **12** and **13**.

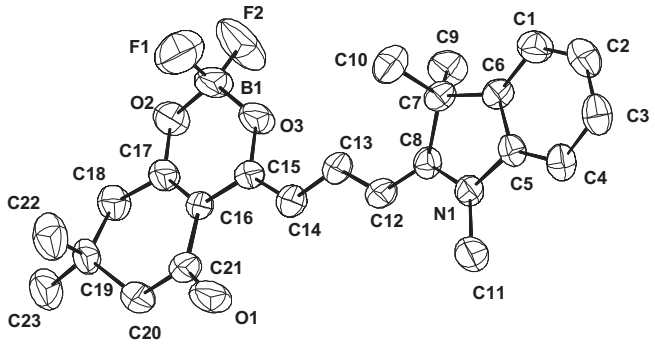

Fig. 2. Molecular structure of **2** (thermal ellipsoids are drawn at the 50% probability level). Selected bond lengths [Å] and angles [°]: F(1)–B(1) 1.389(7), F(2)–B(1) 1.323(6), O(2)–B(1) 1.470(6), O(3)–B(1) 1.440(6), O(2)–C(17) 1.312(4), O(3)–C(15) 1.313(4), C(15)–C(16) 1.444(5), C(16)–C(17) 1.368(5), O(1)–C(21) 1.219(4), C(14)–C(15) 1.383(5), C(13)–C(14) 1.396(5), C(12)–C(13) 1.384(5), C(8)–C(12) 1.378(5); O(2)B(1)O(3) 112.2(4), C(20)C(21)C(16) 118.4(3), C(19)C(20)C(21) 114.3(3).

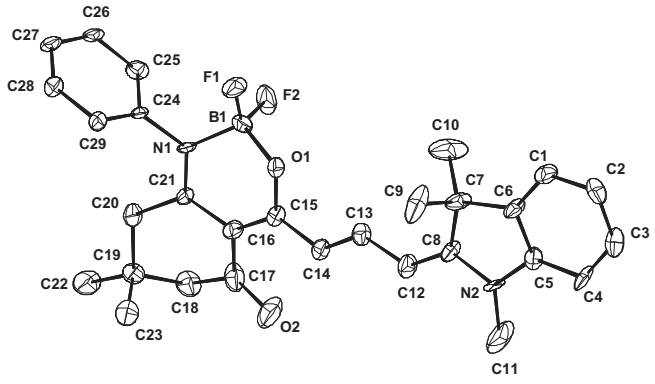

Fig. 3. Molecular structure of **12** (thermal ellipsoids are drawn at the 50% probability level). Selected bond lengths [Å] and angles [°]: F(1)–B(1) 1.377(9), F(2)–B(1) 1.382(8), N(1)–B(1) 1.555(8), N(1)–C(24) 1.438(7), N(1)–C(21) 1.313(9), C(16)–C(21) 1.446(9), C(15)–C(16) 1.409(8), O(1)–C(15) 1.329(8), O(1)–B(1) 1.446(9), C(14)–C(15) 1.417(9), C(13)–C(14) 1.358(8), C(12)–C(13) 1.406(8), C(8)–C(12) 1.388(8), N(2)–C(8) 1.374(8), C(16)–C(17) 1.46(1), O(2)–C(17) 1.23(1); N(1)B(1)O(1) 108.9(6), C(17)C(18)C(19) 109.7(4), C(16)C(17)C(18) 117.8(6).

An alternative structure, with the BF_2 moiety O,O-chelated by two carbonyl groups, could be assumed for complex **11**. To rule it out, we performed X-ray diffraction analysis of the crystals of related dye **12** which unequivocally confirmed the presence of the oxazaborine ring. To compare the oxazaborine dye to its dioxaborine counterpart, the same structural determination was also carried out for the crystals of dye **2.** The respective ORTEP drawings of molecular structures of **2** and **12** are shown in Figs. 2 and 3.

As found by X-ray diffraction, the 6-membered cycle C(16–21) in molecule **2** is not planar (the maximum deviation from the least-squares plane amounts to 0.314 Å). The fragment C(16–18) C(20–21) is almost planar (the average deviation from least-squares plane is 0.001 Å) and the dihedral angle between the C(16–18)C(20–21) and C(18–20) planes is 44.16°. The dihedral angle C(15)C(16)C(21)O(1) is 7.4°. The 6-membered cycle C(16–21) in molecule **12** is not planar and more distorted than the C(16–21) cycle in **2** (the maximum deviation from the least-squares plane amounts to 0.362 Å). The dihedral angle C(15–17)O(2) is 7.9°. The phenyl ring C(24–29) is almost orthogonal to the plane O(1)C(15) C(16)C(21)N(1) (with the average deviation 0.001 Å from the least-squares plane): the dihedral angle C(29)C(24)N(1)C(21) is 84.23°. Due to the conjugation of the N(1) electron pair with the double bond N(1) = C(21), the trigonal-planar bond configuration of N(1) is observed, with the sum of the bond angles 359.4°. The atoms in the polymethine chain C(15)–C(14)–C(13)–C(12)–C(8) are coplanar; the average deviation from the least-squares plane is 0.010 Å in **12** and 0.014 Å in **2**. The pattern and magnitude of the bond length alternation in this conjugated moiety appears to strongly depend on the nature of the chelate ring. As seen from Figs. 2 and 3, the alternation changes the sign and grows in magnitude in going from dye **2** to **12**.

Table 1 demonstrates the spectral properties of oxazaborine merocyanines **7**, **12**, and **13** as well as their dioxaborine analogues **2** and **3** (for comparison) in weakly and strongly polar aprotic solvents (dichloromethane and acetonitrile, respectively), and in a strongly polar protic solvent (formamide). The λ_{max} and λ^f_{max} denote the respective wavelengths of the absorption and fluorescence maxima, ε the molar absorption coefficient, $\Delta\lambda_{max}$ and $\Delta\lambda^f_{max}$ the corresponding spectral shifts with reference to analogous dioxaborine dyes, S the absorption band half-width, $\Delta\nu$ the Stokes shift, and Φ the fluorescence quantum yield.

It is challenging to elucidate the spectral effects of going from the O,O- to N,O-chelated BF_2 moiety in boron-containing heterocyclic dye end groups. To this end, we invoke the concept of ideal polymethinic and polyenic states introduced previously by Daehne on the basis of his triad theory [14]. According to this approach, the π-properties of donor-acceptor (merocyanine) dyes are conveniently treated in terms of three limiting resonance structures referring to the ground state, viz., polyenic non-charge-separated

Table 1
Spectral characteristics of merocyanines **2**, **3**, **7**,[a] **12**, and **13.**

Dye	Solvent	λ_{max} [nm] (ε 10^{-5}, M^{-1} cm^{-1})	$\Delta\lambda_{max}$ [nm]	S [cm^{-1}]	λ^f_{max} [nm]	$\Delta\lambda^f_{max}$ [nm]	$\Delta\upsilon$ [cm^{-1}]	Φ
2	CH_2Cl_2	534 (1.314)	–	1666	556	–	741	0.03
	CH_3CN	532 (1.142)	–	1937	552	–	681	0.01
3	CH_2Cl_2	545 (1.428)	–	992	559	–	460	0.04
	CH_3CN	538 (0.990)	–	1976	555	–	569	0.01
	$HCONH_2$[b]	538 505	–	2674	556	–	602	0.02
7	CH_2Cl_2[b]	545	0	856	559	0	460	0.02
	CH_3CN[b]	538 506	0	2893	555	0	569	>0.01
	$HCONH_2$[b]	505	0	3182	559	3	–	0.01
12	CH_2Cl_2	536 (1.276)	2	1590	569	13	1082	0.65
	CH_3CN	536 (1.251)	4	1722	567	15	1020	0.16
13	CH_2Cl_2	558 (1.516)	13	1207	579	20	650	0.65
	CH_3CN	555 (1.525)	17	1264	576	21	657	0.16
	$HCONH_2$[b]	563	25	1119	582	26	580	0.15

[a] The analogous merocyanine with the indolenine end group could not be obtained.
[b] Quantitative spectra of dyes could not be recorded due to their poor solubility or thermal instability in solution.

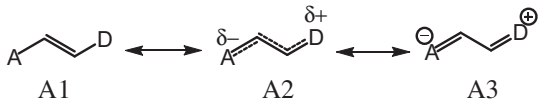

Scheme 5. Resonance structures of donor–acceptor dyes.

A1, polymethinic **A2**, and polyenic charge-separated **A3** (Scheme 5). As predicted by intuition and supported experimentally [15], transitions between the structures are governed by the donor–acceptor strength of end residues and/or solvent polarity. For weak donors and/or acceptors, the type **A1** realizes which is characterized by positive solvatochromism. By increasing the donor–acceptor strength of end substituents to a certain value, the ideal polymethinic structure **A2** is reached which is remarkable for practically full equalization of bond orders, just as in symmetrical cyanine dyes; accordingly, the molecules of the type **A2** are only slightly solvatochromic, if at all (cf. to slight negative solvatochromism of symmetrical cyanines). On further rise of the donor–acceptor strength of end groups, the electronic structure of merocyanines tends from **A2** toward A**3**, the latter exhibiting pronounced negative solvatochromism.

For boron chelate merocyanines, the boron-containing nucleus acts as an acceptor and the other aza heterocyclic end group as a donor.

Comparing the spectral data for dioxaborine dye **3** and oxazaborine dye **7**, both containing the benzothiazole nucleus as the second end group, it is seen that substitution of the 3-O atom by the NH group in the chelate ring has almost no effect on absorption and fluorescence band positions as well as fluorescence intensity. At the same time, compound **7** is more readily solvated due to the presence of the NH group, which, in turn, causes the strong intensity redistribution between the 0–0 and 0–1 vibronic absorption bands.

Figs. 4 and 5 demonstrate the absorption spectra of merocyanines **3** and **7** in various solvents. Negative solvatochromism of dye **3** (see Table 1) suggests that this compound is structurally between the types A2 and A3. Accordingly, it tends to A2 with decreasing solvent polarity. Vice versa, switching from acetonitrile to formamide brings the molecular structure closer to A3 and not

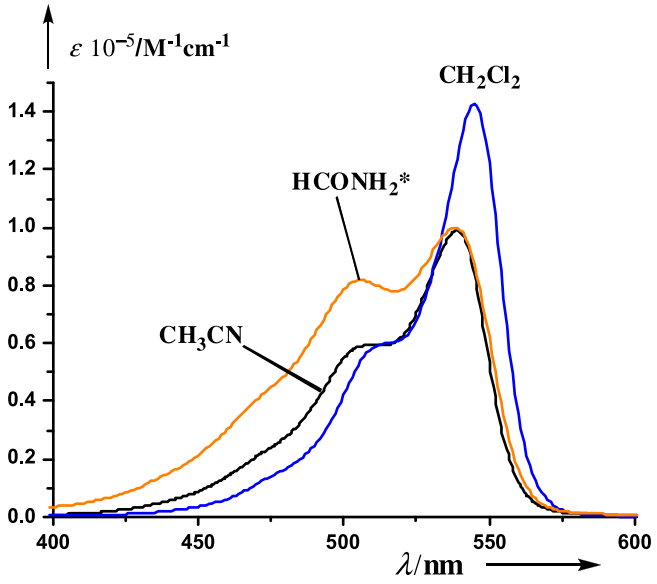

Fig. 4. Absorption spectra of dye **3** (the star denotes qualitative measurement).

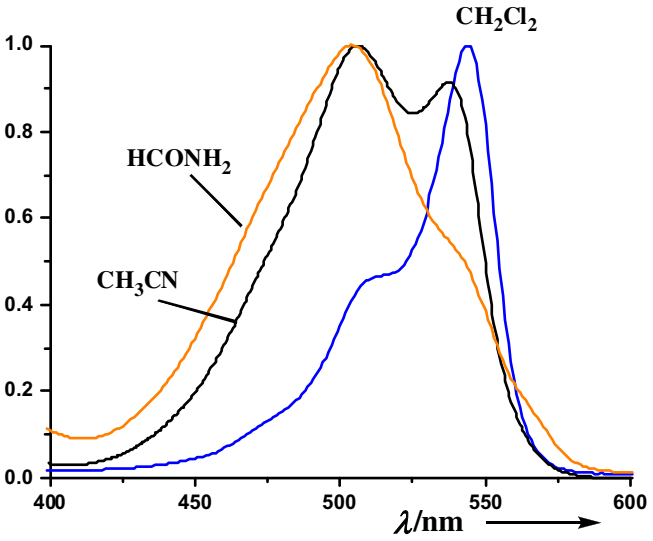

Fig. 5. Normalized absorption spectra of dye **7**.

only due to an increase in the solvent dielectric constant but also as a result of dye-formamide H-bonding through the unchelated carbonyl group of merocyanine **3**. One can also assume, by analogy with previously reported studies [15a], that another effect of H-bonding is the enhanced 0–1 vibronic absorption peak (which is identified by its 1181 cm^{-1} shift from the 0–0 transition band).

Replacing the NH group for the O-atom in the chelate ring, i.e., going from dye **3** to **7**, gives rise to the second centre of H-bonding of dye molecules by highly polar solvents (e.g., formamide) thus leading to an inverse intensity distribution between the 0–0 and 0–1 vibronic bands (cf. to the identical absorption band shapes of **3** and **7** in weakly polar aprotic dichloromethane) Scheme 6. Like cyanines [16], dyes **3** and **7** tending to the polyenic charge-separated structure **A3** are characterized by much weaker specific solvation in the excited than in the ground state and, hence, by much less pronounced solvation effects on fluorescence than on absorption (though solvents, of course, influence the electron density distribution in dye molecules). This is evident from the comparison of the absorption and fluorescence band shapes for dyes **3** and **7** (cf. Fig. 4 with Fig. 6 and Fig. 5 with Fig. 7), also taking into account the fluorescence excitation band shapes for dye 7 (see Fig. 8).

It is seen that the bands in the fluorescence and fluorescence excitation spectra are narrower and more structured than in the absorption spectra, without a strong 0–1 vibronic peak. The fluorescence excitation spectra of dye **7** allow to implicitly assess the

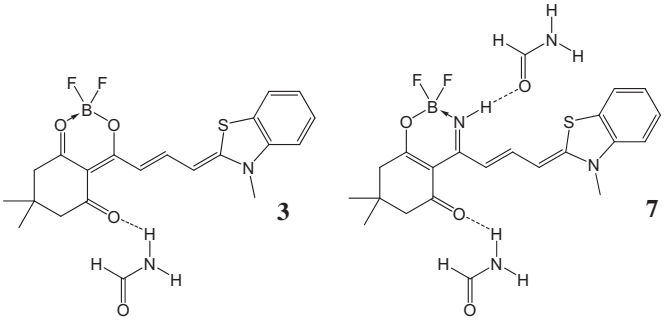

Scheme 6. Probable solvatation of dyes **3** and **7** by formamide.

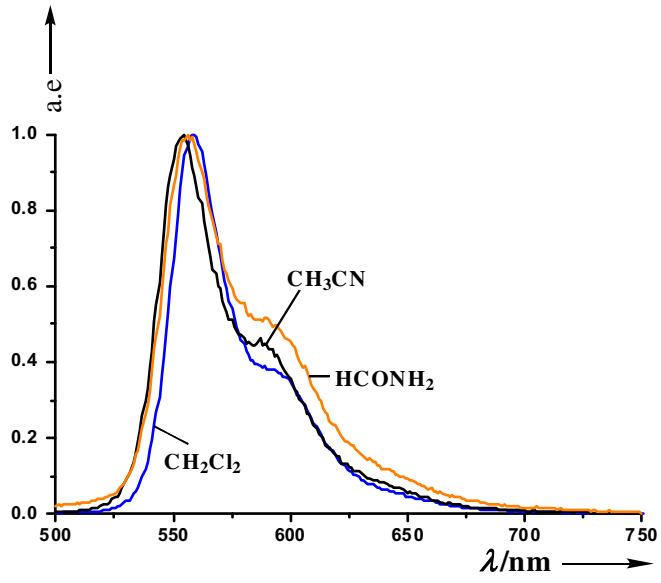

Fig. 6. Fluorescence spectra of dye **3**.

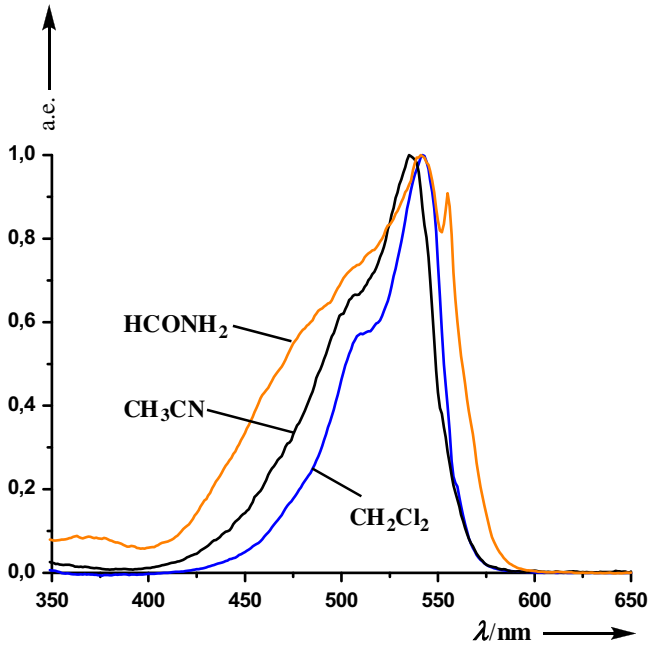

Fig. 8. Fluorescence excitation spectra of dye **7**.

absorption of the unsolvated compound; as expected, they are mirror images of the corresponding fluorescence spectra. Due to the presence of an additional H-bonding centre, oxazaborine dye **7** is more sensitive to the action of polar solvents than its dioxaborine analogue **3** (see above) and, accordingly, exhibits a broader fluorescence band in formamide.

Now consider the spectral properties of the dyes derived from oxazaborine **11** in which the 1-O atom of the dioxaborine ring is substituted by the NPh group. Comparing the spectral characteristics of dyes **2** and **3** to those of **12** and **13**, respectively (see Table 1), one can see that going from the O,O- to N,O-chelate ring is accompanied by a bathochromic effect, slight for indolenine dyes (2–4 nm for absorption and 13–15 nm for fluorescence) and more pronounced for their benzothiazole analogues (13–25 and 20–26 nm). Interestingly, negative solvatochromism of oxazaborine dyes **12** and **13** (respective blue shifts of 0 and 3 nm on passing from dichloromethane to acetonitrile) almost vanishes as compared to their dioxaborine counterparts (2 and 7 nm) and even changes its sign to positive in some media (a red shift of 5 nm for **13** on passing from dichloromethane to formamide) (Fig. 9). Moreover, **12** and **13** show a some tendency towards absorption band narrowing relative to the corresponding dioxaborine dyes **2** and **3** (except dye **13** in dichloromethane), in contrast to what is observed for dye **7** vs. **3** except their dichloromethane solutions (trace the values *S* in Table 1). The trends in fluorescence spectra are quite similar (cf. Fig. 6 with Fig. 10). All these features consistently suggest that dyes **12** and **13**, though falling in the same negatively solvato(fluoro)chromic region **A2**–**A3** as dyes **2**, **3** and **7**, are closer to the polymethinic type **A2** and can, under certain conditions, move to the region **A1**–**A2** accordingly changing the sign of solvato(fluoro)chromism. The specificity found is likely the result from

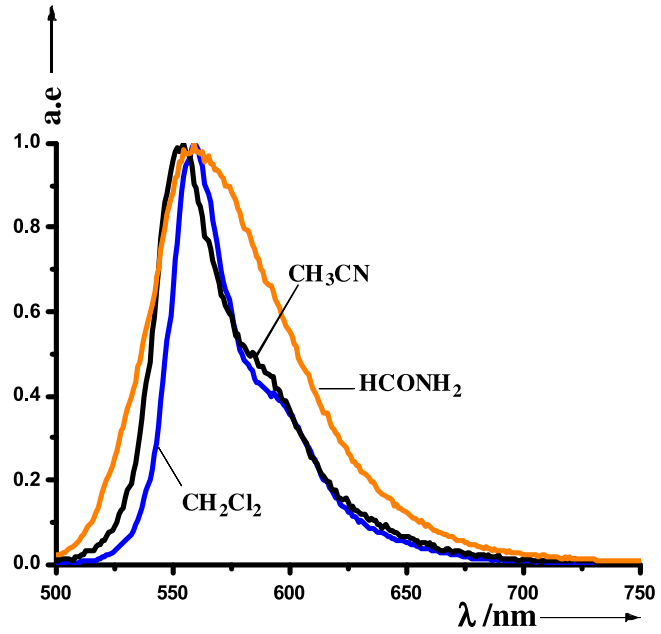

Fig. 7. Fluorescence spectra of dye **7**.

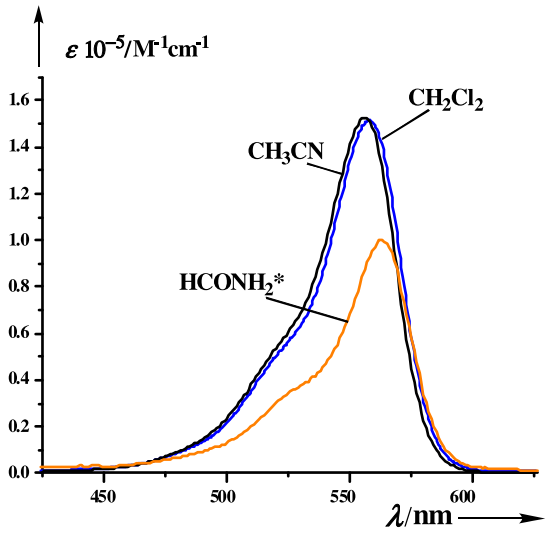

Fig. 9. Absorption spectra of dye **13** (the star denotes qualitative measurement).

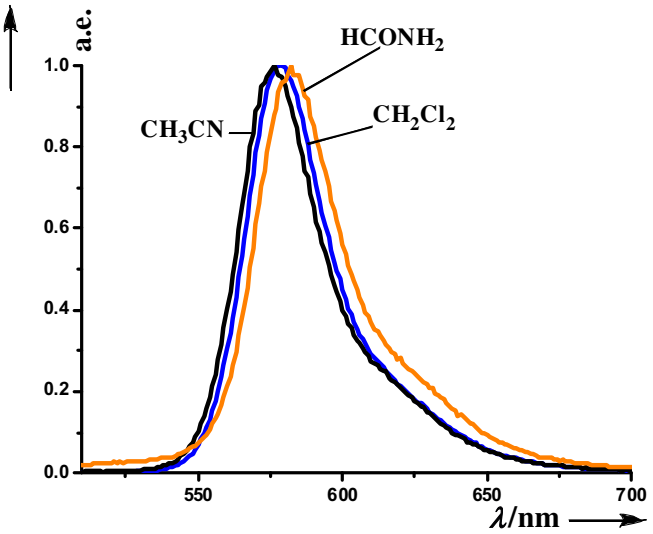

Fig. 10. Fluorescence spectra of dye **13**.

the lower electron-acceptor strength of N,O-chelate nucleus **11** than that of its O,O analogue **1** or N,O-chelate **6** with the isomeric position of the N atom. This assumption is also corroborated by the X-ray analytical data for compounds **2** and **12** presented in Figs. 2 and 3: in the solid state, a smaller bond alternation in the polymethine chain of **2** suggests that it is closer than **12** to the ideal polymethinic bond-equalized type **A2** (whereas the opposite is inferred for the dissolved dyes from the magnitudes of their solvatochromism). As indicated by the opposite alternation patterns of the two compounds, they are positioned on different sides of **A2**: charge-separated dye **2** in the region **A2**–**A3** and non-charge-separated dye **12** in **A1**–**A2**. Going from the former to the latter region implies a decrease in the donor–acceptor strength of end substituents (in our case, a weakening of the acceptor character of the chelate ring). Another evidence of the decreased acceptor strength of the NPh-substituted chelate is provided by the ab initio calculated frontier MO energies of dyes **2** and **12**: they are noticeably higher for the latter, as shown in Fig. 11.

As found, substitution of the 1-O ring atom by the NPh group leads to a drastic 10–20-fold increase in the fluorescence efficiency of the corresponding merocyanines irrespective of solvent polarity (cf. respective Φ values for dyes **2**, **3** and **12**, **13** in Table 1). Unlike the previously reported cases when going from alkyl to (het)aryl

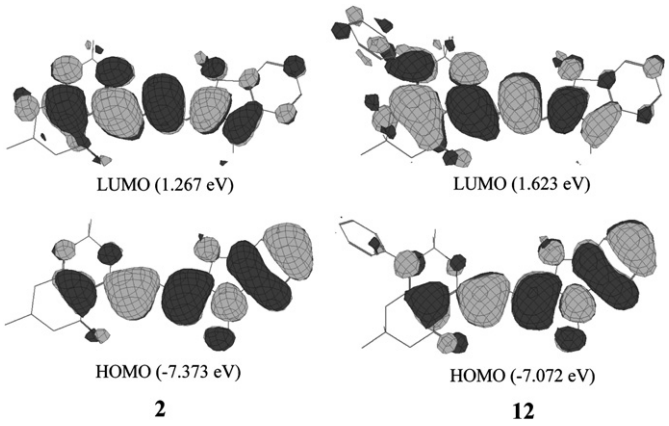

Fig. 11. HOMO and LUMO energies and shapes for **2** and **12** determined at the UHF/6-31G** level of theory. (The molecular geometry is based on X-ray analytical data).

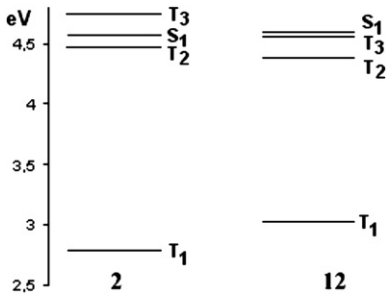

Fig. 12. Excited singlet and triplet state energies in dyes **2** and **12** obtained at the RHF/6-31G** level of theory, with 10 occupied and 10 virtual MOs included in the configuration interaction space.

substituents in heterocyclic systems led to large Stokes shifts and high quantum yields of the resulting molecules due to their excited-state planarization [17], here we can hardly attribute the enhancement of fluorescence to the specific effects of the phenyl group. First, the 84°-degree twisted phenyl ring participates very slightly in the frontier π-MOs which are mainly involved in the first electronic transition (see Figs. 3 and 11). Second, this group is unlikely to achieve significant coplanarization with the rest of the molecule in the relaxed S_1 state, since the Stokes shifts of **12** and **13** are only a little, if at all, larger than those of **2** and **3**, respectively (see Table 1).

We have also suggested intersystem crossing, a possible channel of the fluorescence quenching, to be present in dye **2** and absent in **12**. However, the calculated energies of the excited singlet and triplet states do not support this assumption, since S_1 depopulation via the close-lying triplet state(s) appears even more probable in the oxazaborine than in the dioxaborine merocyanine (see Fig. 12).

As another plausible explanation for the enhanced fluorescence of dyes **12** and **13** compared to **2** and **3** (and also to most of the merocyanines [18]), we can assume that the oxazaborine dyes have a reduced probability for the S_0–S_1 conical intersections associated with bond twisting. Conical intersections causing photoisomerizations or radiationless returns of reagents to the initial S_0 state act as photochemical funnels; a driving force for their occurrence is, as a rule, a S_1 potential surface curvature in the vicinity of the Franck–Condon region caused by electron density localization in certain parts of the excited molecule (this is typical of push-pull merocyanines as well as of short polymethines) [19]. It can be that substitution of the 1-O ring atom by the less electron-acceptor NPh group in the chelate merocyanines concerned leads to a flattened S_1 potential surface thereby preventing the interstate conical intersection in dyes **12** and **13**.

3. Conclusion

We have first synthesized the 3-aza and 1-aza analogues of 2,2-difluoro-1,3,2(2*H*)dioxaborines as well as two series of the corresponding oxazaborine merocyanines and studied the spectroscopic effects of the O-to-N substitution in both dye types. As found, 3-NH oxazaborine dyes have much the same absorption and fluorescence band positions as the corresponding dioxaborine compounds but exhibit different absorption band shapes (as a result of the enhanced solvation and hence the intensity redistribution between the 0–0 and 0–1 vibronic absorption peaks). Contrastingly, 1-NPh oxazaborine merocyanines are characterized by a red shift in absorption and fluorescence, and also by more than one order increase in the fluorescence quantum yield.

4. Experiment

Frontier molecular orbital energies as well as energies of the excited singlet and triplet states for dye **2** and **12** were determined by standard ab initio calculations with the aid of the HyperChem. Package. ^{1}H NMR spectra were obtained with Varian VXR 300 and Varian Gemini 2000 instruments at 300 and 400 MHz, respectively, using TMS as internal reference. Electronic absorption spectra were recorded on a Shimadzu UV-3100 spectrophotometer. Fluorescence and fluorescence excitation spectra were taken on a Cary Eclipse instrument and were fully corrected. The fluorescence quantum yields (Φ) of dyes were determined by a known method [20] relative to Rhodamine 6 G ($\Phi = 0.95$ in EtOH).

4.1. Oxazaborine **4**

Aniline (0.91 ml, 10 mmol) was added to a suspension of dioxaborine **1** (2.3 g, 10 mmol) and benzene (15 ml). The mixture was heated with a Dean-Stark trap at reflux for 5 h, allowed to cool to room temperature, and left for 12 h. The solid was filtered off, washed with benzene (2 × 10 ml), and recrystallized from *i*-PrOH. Yield 2.32 g (76%); m.p. 131 °C; ^{1}H NMR (300 MHz, $CDCl_3$, 25 °C): $\delta = 1.14$ (s, 6H, $2CH_3$), 2.44 (s, 5H, $CH_3 + CH_2$), 2.71 (s, 2H, CH_2), 7.18 (d, ^3J(H,H) = 8.0 Hz, 2H, ArH); 7.40–7.57 ppm (m, 3H, ArH); elemental analysis calcd (%) for $C_{16}H_{18}BF_2NO_2$: C 62.98, H 5.95, N 4.59; found: C 63.12, H 6.06, N 4.69.

4.2. Oxazaborine **6**

A mixture of enamine **5** [21] (1.0 g, 5.5 mmol) and boron trifluoride etherate (1.4 ml, 11 mmol) was heated at 100 °C for 0.5 h and an additional portion of boron trifluoride etherate (0.5 ml, 3.9 mmol) was added. On elevating the temperature to 150 °C, the mixture was heated for 1 h and then allowed to cool to room temperature. After the system had been evaporated to remove volatile reagents and products, the residue was extracted by boiling diethyl ether (5 × 10 ml). The extract was evaporated and the precipitate was recrystallized from diethyl ether. Yield 0.8 g (63%); m.p. 142 °C; ^{1}H NMR (300 MHz, $CDCl_3$, 25 °C): $\delta = 1.10$ (s, 6H, $2CH_3$), 2.39 (s, 2H, CH_2), 2.67 (s, 2H, CH_2), 2.70 (s, 3H, CH_3), 7.79 ppm (br. s. 1H, NH); elemental analysis calcd (%) for $C_{10}H_{14}BF_2NO_2$: C 52.44, H 6.16, N 6.12; found: C 52.56, H 6.21, N 6.05.

4.3. Merocyanine **7**

A mixture of oxazaborine **6** (0.1 g, 0.44 mmol), 3-methyl-3*H*-benzothiazole-2-ylidene)acetaldehyde (0.083 g, 0.44 mmol), and acetic anhydride (1 ml) was heated at 75 °C for 15 min. After cooling to room temperature, diethyl ether (20 ml) was added and the resulting mixture was allowed to stand for 30 min. The precipitate was filtered off, washed with diethyl ether (2 × 10 ml), and recrystallized from CH_3CN. Yield 0.058 g (32%); m.p. 211 °C; ^{1}H NMR (400 MHz, $CDCl_3$, 25 °C): $\delta = 1.09$ (s, 6H, $2CH_3$), 2.38 (s, 2H, CH_2), 2.61 (s, 2H, CH_2), 3.74 (s, 3H, NCH_3), 6.22 (d, ^3J(H,H) = 13.4 Hz, 1H, H_α), 7.32–7.43 (м, 3H, 2ArH + H_γ), 7.51 (t, ^3J(H,H) = 7.8 Hz, 1H, ArH), 7.69 (d, ^3J(H,H) = 7.8 Hz, 1H, ArH), 8.53 ppm (t, ^3J(H,H) = 13.4 Hz, 1H, H_β); elemental analysis calcd (%) for $C_{20}H_{21}BF_2N_2O_2S$: C 59.72, H 5.26, N 6.96; found: C 60.02, H 5.19, N 6.92.

4.4. Complex **9**

A mixture of enamine **8** [22] (1.0 g, 5.5 mmol) and boron trifluoride etherate (2.1 ml, 16.5 mmol) was heated at 100 °C for 0.5 h. After cooling to room temperature, boron trifluoride etherate (0.5 ml, 3.9 mmol) in dichlorobenzene (10 ml) was added. The obtained mixture was heated at reflux for 4 h and allowed to cool to room temperature. The resulting solid was suspended in diethyl ether (20 ml). The precipitate was filtered off and washed with diethyl ether (3 × 15 ml). The crude product was dissolved in MeOH (5 ml) and the solid was filtered off. Diethyl ether (30 ml) was added to the filtrate, followed by filtering off the precipitate and washing it with diethyl ether (2 × 10 ml). Yield 0.6 g (43%); m.p. 194 °C; ^{1}H NMR (300 MHz, [D_6]DMSO, 25 °C): $\delta = 0.95$ (s, 6H, $2CH_3$), 2.17 (s, 2H, CH_2), 2.35 (s, 3H, CH_3), 2.47 (s, 2H, CH_2), 8.72 (br. s. 1H, NH), 10.82 ppm (br. s. 1H, NH); elemental analysis calcd (%) for $C_{10}H_{15}BF_3NO_2$: C 48.23, H 6.07, N 5.62; found: C 48.77, H 6.00, N 5.43.

4.5. Oxazaborine **11**

A mixture of enamine **10** [23] (1.24 g, 5 mmol) and boron trifluoride etherate (0.76 ml, 6 mmol) was heated at 80 °C for 1 h and then allowed to cool to room temperature. The resulting solid was suspended in diethyl ether (30 ml) and then the ether layer was removed. The crude product was suspended in *i*-PrOH (20 ml), followed by filtering off the obtained precipitate, washing it twice with *i*-PrOH (10 ml), and recrystallization from *i*-PrOH. Yield 0.64 g (42%); m.p. 176 °C; ^{1}H NMR (300 MHz, $CDCl_3$, 25 °C): $\delta = 0.98$ (s, 6H, $2CH_3$), 2.24 (s, 2H, CH_2), 2.39 (s, 2H, CH_2), 2.76 (s, 3H, CH_3), 7.17 (d, ^3J(H,H) = 6.6 Hz, 2H, ArH), 7.41–7.52 ppm (м, 3H, ArH). elemental analysis calcd (%) for $C_{16}H_{18}BF_2NO_2$: C 62.98, H 5.95, N 4.59; found: C 62.90, H 5.93, N 4.63.

4.6. Merocyanines **12**, **13**. General procedure

Acetic anhydride (0.5 ml) was added to a mixture of compound **11** (0.25 g, 0.8 mmol) and Fisher's aldehyde (0.16 g, 0.8 mmol) or 3-methyl-3*H*-benzothiazole-2-ylidene)-acetaldehyde (0.15 g, 0.8 mmol). The obtained mixture was heated at 100 °C for 0.5 h and then allowed to cool to room temperature. After addition of diethyl ether (20 ml), the mixture was left for 1 h. The precipitate was filtered off, washed twice with ether (30 ml), and recrystallized from CH_3CN.

4.6.1. Merocyanine **12**

Yield 0.11 g (25%); m.p. 294 °C; ^{1}H NMR (300 MHz, $CDCl_3$, 25 °C): $\delta = 0.98$ (s, 6H, $2CH_3$), 1.66 (s, 6H, $2CH_3$), 2.28 (s, 2H, CH_2), 2.36 (s, 2H, CH_2), 3.34 (s, 3H, NCH_3), 5.85 (d, ^3J(H,H) = 13.5 Hz, 1H, H_α), 6.86 (d, ^3J(H,H) = 7.5 Hz, 1H, ArH), 7.06 (t, ^3J(H,H) = 6.9 Hz, 1H, ArH), 7.17–7.51 (m, 7H, ArH), 7.64 (d, ^3J(H,H) = 13.5 Hz, 1H, H_γ), 8.59 ppm (t, ^3J(H,H) = 13.5 Hz, 1H, H_β); elemental analysis calcd (%) for $C_{29}H_{31}BF_2N_2O_2$: C 71.31, H 6.40, N 5.74; found: C 71.65, H 6.59, N 5.82.

4.6.2. Merocyanine **13**

Yield 0.10 g (29%); m.p. 258 °C; ^{1}H NMR (300 MHz, $CDCl_3$, 25 °C): $\delta = 0.97$ (s, 6H, $2CH_3$), 2.27 (s, 2H, CH_2), 2.36 (s, 2H, CH_2), 3.56 (s, 3H, NCH_3), 5.99 (d, ^3J(H,H) = 13.6 Hz, 1H, H_α), 7.10–7.25 (m, 3H, ArH), 7.34–7.56 (m, 6H, ArH), 7.65 (d, ^3J(H,H) = 13.6 Hz, 1H, H_γ), 8.31 ppm (t, ^3J(H,H) = 13.6 Hz, 1H, H_β); elemental analysis calcd (%) for $C_{26}H_{25}BF_2N_2O_2S$: C 65.28, H 5.27, N 5.86; found: C 65.19, H 5.37, N 5.94.

4.7. X-ray structure determination for **2** and **12**

Crystals of **2** and **12** suitable for X-ray diffraction analysis were grown slowly from a saturated dye solution in *i*-PrOH and acetonitrile, respectively.

Crystals of **2**: $C_{23}H_{26}B_1F_2N_1O_3$; $M = 413.27$; system: monoclinic, space group: $P2_1/c$ (N 14); unit-cell dimensions: $a = 9.636(1)$,

$b = 16.562(2)$, $c = 14.445(1)$ Å, $\beta = 107.679(4)^\circ$, $V = 2196.4(4)$ Å^3, $Z = 4$, calculated density: 1.250 g cm^{-3}, $\mu(\text{MoK}\alpha) = 0.092$ mm^{-1}, $F(000) = 872$.

Crystals of **12**: $C_{29}H_{31}B_1F_2N_2O_2$; $M = 488.38$; system: monoclinic, space group *Cc* (N9); unit-cell dimensions: $a = 16.034(4)$, $b = 15.491(5)$, $c = 10.250(3)$ Å, $\beta = 94.43(1)^\circ$, $V = 2538.1(1)$Å^3, $Z = \varphi 4$, calculated density: 1.278 g cm^{-3}, $\mu(\text{MoK}\alpha) = 0.089$ mm^{-1}, $F(000) = 1032$.

The intensities of 24,817 (**2**) and 5836 (**12**) reflections were measured at room temperature on a Bruker Smart Apex II diffractometer operating in the ω and scans mode. 4500 (**2**) and 3336 (**12**) unique reflections [$R_{\text{int}} = 0.066$ (**2**), 0.073 (**12**)] were used in further refinement. Data were corrected for Lorentz and polarization effects. The structure was solved by direct methods and refined by the full-matrix least-squares technique in the anisotropic approximation for non-hydrogen atoms using the SHELXS97 and SHELXL97 programs [24], and CRYSTALS program package [25]. Hydrogen atoms were located in the difference Fourier maps and refined with fixed positional and thermal parameters. The Chebyshev weighting scheme was used. The SADABS [26] absorption correction was applied. For **2**, the refinement converged to $R_w = 0.035$, $R_1 = 0.038$, GOF = 1.135 for observed 1276 reflections with $I > 3\sigma(I)$ (obsd./var. = 4.7); for **12**, to $R_w = 0.061$, $R_1 = 0.060$, GOF = 0.687 for observed 1781 reflections with $I > 2.5\sigma(I)$ (obsd./var. = 5.44). CCDC reference number is 777793 for **2** and 777794 for **12**.

Atomic coordinates, bond lengths, bond angles, and thermal parameters have been deposited at the Cambridge Crystallographic Data Centre (CCDC). These data can be obtained free of charge *via* www.ccdc.cam.uk/conts/retrieving.html (or from the CCDC, 12 Union Road, Cambridge CB2 1EZ, UK; fax: +44 1223 336 033; or deposit@ccdc.cam.ac.uk). Any request to the CCDC for data should quote the full literature citation and CCDC reference numbers.

Acknowledgements

The authors are grateful to Prof. A.A. Ishchenko and Prof. A.D. Kachkovskii for helpful discussions. The authors thank Prof. S.N. Yarmoluk and Dr. M.Yu. Losytskii for help in carrying out fluorescence measurements.

References

[1] (a) Hales JW, Zheng S, Barlow S, Marder SR, Perry JW. Bisdioxaborine polymethines with large third-order nonlinearities for all-optical signal processing. J Am Chem Soc 2006;128:11362–3;
(b) HCh Lin, Kim HG, Barlow S, Hales JM, Perry JW, Marder SR. Synthesis and linear and nonlinear optical properties of metal-terminated bis(dioxaborine) polymethines. Chem Commun 2011;47:782–4.

[2] (a) Domercq B, Grasso C, Maldonado J-L, Halik M, Barlow S, Marder SR, et al. Electron-transport properties and use in organic light-Emitting diodes of a bis(dioxaborine)fluorene derivative. J Phys Chem B 2004;108:8647–51;
(b) Risko C, Zojer E, Brocorens P, Marder SR, Brédas J-L. Bis-aryl substituted dioxaborines as electron-transport materials: a comparative density functional theory investigation with oxadiazoles and siloles. Chem Phys 2005;313:151–7;
(c) Fabian J, Hartmann H. 1,3,2-Dioxaborines as potential components in advanced materials - a theoretical study on electron affinity. J Phys Org Chem 2004;17:359–69;
(d) Halik M, Schmid G, Davis L. Infineon Technologies AG, DE Pat 10152938; 2002;
(e) Hartmann H, Hunze A, Kanitz A, Rogler W, Rohde D. Osram Opto Semiconductors GmbH, US Pat 7026490B2; 2006.

[3] (a) Halik M, Wenseleers W, Grasso C, Stellacci F, Zojer E, Barlow S, et al. Bis(dioxaborine) compounds with large two-photon cross sections, and their use in the photodeposition of silver. Chem Commun 2003;13:1490–1;
(b) Zojer E, Wenseleers W, Pacher P, Barlow S, Halik M, Grasso C, et al. Limitations of essential-state models for the description of two-photon absorption proceses: the example of bis(dioxaborine)-substituted chromophores. J Phys Chem B 2004;108:8641–6.

[4] Zyabrev K, Doroshenko A, Mikitenko E, Slominskii Y, Tolmachev A. Design, synthesis, and spectral luminescent properties of a novel polycarbocyanine series based on the 2,2-difluoro-1,3,2-dioxaborine nucleus. Eur J Org Chem 2008;9:1550–8.

[5] Halik M, Hartmann H. Synthesis and characterization of new long-wavelength-absorbing oxonol dyes from the 2,2-difluoro-1,3,2-dioxaborine type. Chem Eur J 1999;5:2511–7.

[6] Gerasov AO, Shandura MP, Kovtun YP. Series of polymethine dyes derived from 2,2-difluoro-1,3,2-(2H)-dioxaborine of 3-acetyl-7-diethylamino-4-hydroxycoumarin. Dyes Pigm 2008;77:598–607.

[7] Traven VF, Chibisova TA, Manaev AV. Polymethine dyes derived from boron complexes of acetylhydroxycoumarins. Dyes Pigm 2003;58:41–6.

[8] (a) Tyutyulkov N, Fabian J, Mehlhorn A, Dietz F, Tadjer A. Polymethene dyes. Structure and properties. Sofia: St. Kliment Ohridski Univ Press; 1991;
(b) Griffiths J. Colour and constitution of organic molecules. Academic Press; 1976;
(c) Fabian J, Hartmann H. Light absorption of organic colorants. Springer-Verlag; 1980.

[9] (a) Xia M, Wu B, Xiang G. Synthesis, structure and spectral study of two types of novel fluorescent BF_2 complexes with heterocyclic 1,3-enaminoketone ligands. J Fluor Chem 2008;129:402–8;
(b) Zhou Y, Xiao Y, Chi S, Qian X. Isomeric boron–fluorine complexes with donor–acceptor architecture: strong solid/liquid fluorescence and large stokes shift. Organic Lett 2008;10:633–6.

[10] Zyabrev KV, Ilchenko AY, Slominskii YL, Tolmachev AI. Polymethine dyes based on 2,2-difluoro-1,3,2-dioxaborine complex, synthesized from 2-acetyldimedone. Ukr Khim Zh 2006;72:56–63.

[11] Vasil'ev LS, Azarevich OG, Bogdanov VS, Bochkareva MN, Dorokhov VA. Boron chelates with 5,5,5-trifluoro- and 5,5,5-trichloro-4-aminopent-3-en-2-ones. Russ Chem Bull 1992;41:2104–7.

[12] Tolmachev AI, Derevyanko NA, Karaban EF, Kudinova MA, Pyrylocyanines VI. Conversion of 4-pyrylocyanines to 4-pyridocyanines. Chem Heterocycl Compd 1975;11:534–8.

[13] VanAllen JA, Reynolds GA. The reactions of 2,2-difluoro-4-methylnaphtho[l,2-e]-1,3,2-dioxaborine and its [2,1-e] isomer with carbonyl compounds and with aniline. J Heterocycl Chem 1969;6:29–35.

[14] Bach G, Daehne S. RODD'S chemistry of carbon compounds. 2nd suppl. to 2nd ed., vol IVB. Amsterdam: Elsevier Science; 1997. Chap 15, Het. Comp., p. 383.

[15] (a) Kulinich AV, Derevyanko NA, Ishchenko AA. Synthesis, structure, and solvatochromism of merocyanine dyes based on barbituric acid. Russ J Gen Chem 2006;76:1441–57;
(b) Kulinich AV, Derevyanko NA, Ishchenko AA. Electronic structure and solvatochromism of merocyanines based on *N*, *N*-diethylthiobarbituric acid. J Photochem Photobiol A 2007;188:207–17;
(c) Kulinich AV, Ishchenko AA, Groth UM. Electronic structure and solvatochromism of merocyanines NMR spectroscopic point of view. Spectrochim Acta Part A 2007;68:6–14.

[16] Ishchenko AA. Structure and spectral luminescent properties of polymethine dyes. Kiev: Naukova Dumka; 1994.

[17] (a) Przhonskaya OV, Tikhonov EA. Structure of polymethine dyes' molecules and their lasing properties. Opt Spektrosk 1978;44:480–5;
(b) Pozharskii AF, Chegolya TN, Simonov AM. The nature of the interaction of the phenyl and imidazole rings in the N-arylimidazoles. Chem Heterocycl Compd 1968;4:373–4;
(c) Lifshits EB, Shagalova DY, Yagupolskii LM. About properties and structure of 1,1′-3,3′-tetraethyl- and 1,1′-diphenyl-3,3′ diethylimidacarbocyanines substituted into the heterocyclic residue. J Sci Appl Photog Cinematogr 1979;24:140–2;
(d) Knyazhanskii MI, Tymyanskii YR, Feigelman VM, Katritsky AR. Pyridinium salts: luminescent spectroscopy and photochemistry. Heterocycles 1987;26:2963–82.

[18] (a) Ishchenko AA, Kulinich AV, Bondarev SL, Knyukshto VN. Photodynamics of polyene-polymethine transformations and spectral fluorescent properties of merocyanine dyes. J Phys Chem A 2007;111:13629–37;
(b) Kulinich AV, Derevyanko NA, Ishchenko AA, Bondarev SL, Knyukshto VN. Structure and fluorescent properties of merocyanines based on N, N-diethylthiobarbituric acid. J Photochem Photobiol A 2008;197:40–9;
(c) Kulinich AV, Derevyanko NA, Ishchenko AA, Bondarev SL, Knyukshto VN. Structure and fluorescent properties of indole cyanine and merocyanine dyes with partially locked polymethine chain. J Photochem Photobiol A 2008;200:106–13.

[19] (a) Sanchez-Galvez A, Hunt P, Robb MA, Olivucci M, Vreven T, Schlegel HB. Ultrafast radiationless deactivation of organic dyes: evidence for a two-state two-mode pathway in polymethine cyanines. J Am Chem Soc 2000;122:2911–24;
(b) Xu XF, Kahan A, Zilberg S, Haas Y. Photoreactivity of a push-pull merocyanine in static electric fields: a three-state model of isomerization reactions involving conical intersections. J Phys Chem 2009;113:9779–91;
(c) Olsen S, McKenzie RH. Conical intersections, charge localization, and photoisomerization pathway selection in a minimal model of degenerate monomethine dye. J Chem Phys 2009;131:234306.

[20] Fery-Forgues S, Lavabre D. Are fluorescence quantum yields so tricky to measure? A demonstration using familiar stationery products. J Chem Educ 1999;76:1260–4.

[21] Crossley AW, Renouf N. Acyl derivatives of the dihydroresorcins. Part I. The action of hydroxylamine and phenylhydrazine on C-acetyldimethyl- and C-acetyltrimethyl-dihydroresorcins. J Chem Soc 1912;101:1524–38.
[22] Akhrem AA, Moiseenkov AM, Lakhvich FA. Synthesis and some properties of 3-chloro-2-acetyl-2-cyclohexen-1-ones. Russ Chem Bull 1971;20:2642–5.
[23] Tamura Y, Fukumori S, Wada A, Okuyama S, Adachi J, Kita Y. Photochemical dealkylation of 2-acyl-3-alkylamino-5,5-dimethyl-2-cyclohexen-1-ones. Chem Pharm Bull 1982;30:1692–6.
[24] (a) Sheldric GM. SHELXS97-Program for the solution of crystal structure. Germany: University of Göttingen; 1997;
(b) Sheldric GM. SHELXL97-Program for the refinement of crystal structures. Germany: University of Göttingen; 1997.
[25] Watkin DJ, Prout CK, Carruthers JR, Betteridge PW. CRYSTALS, Issue 10. Chemical Crystallography Laboratory, University of Oxford; 1996.
[26] Sheldrick GM. SADABS – Program for scaling and correction of area detector data. Germany: University of Göttingen; 1996.